Progress In Electromagnetics Research B, Vol. 49, 107–127, 2013

A TEMPORAL MULTI-FREQUENCY ENCODING TECHNIQUE FOR CHIPLESS RFID BASED ON C-SECTIONS

Raji S. Nair*, Etienne Perret, and Smail Tedjini

Grenoble-INP/LCIS, 50, rue Barthélémy de Laffemas, BP 54, 26902 Valence Cedex 9, France

Abstract—A time domain chipless RFID tag based on cascaded microstrip coupled transmission line sections (C-sections), which can operate in multi-frequency bands is presented. The group delay characteristics of the C-sections are exploited to generate the tag Identification (ID). The tag comprises cascaded commensurate group of C-sections and two cross-polarized ultra wide-band (UWB) antennas. Since the proposed tag can operate in multi-frequency bands, this paper proves the possibility of increasing the coding capacity compared to the existing time domain designs. A tag operating at ISM (Industrial Scientific and Medical) bands at 2.45 GHz and 5.8 GHz together with conformance of frequency and power regulations is discussed elaborately. The prototype of the device is fabricated and validated experimentally. The time domain characteristic of the tag is also validated experimentally by interrogating a short pulse. Furthermore, measurement results using commercial Ultra Wide Band (UWB) radar which can be used as a chipless RFID reader is also incorporated. The obtained results confirm the concept and the possibility of using temporal multi-frequency in chipless RFID.

1. INTRODUCTION

Time domain chipless RFID has a greater importance while considering frequency regulations into account. Chipless RFID systems should be compatible with the existing standards of Federal Communications Commission (FCC) and European Telecommunications Standards Institute (ETSI), in terms of allocation of frequency and emission power. The existing devices based on frequency approach consume large bandwidth to encode more bits and not suitable with the existing

Received 15 November 2012, Accepted 16 February 2013, Scheduled 18 February 2013
* Corresponding author: Raji Sasidharan Nair (raji.nair@lcis.grenoble-inp.fr).

FCC regulations [1–3]. This can be mitigated using short narrow band pulses, i.e., using UWB standard as in the case in a UWB radar. However, due to low power level, the reading range is of the order of 50 cm [1, 3–5].

For applications with large read-range and low coding capacity, the ISM bands can be employed. Such a scheme remains compatible with the use of a temporal approach. In ISM bands, the allowed emission power is more which leads to high reading range. A good example is the SAW (Surface Acoustic Wave) tag developed by RFSAW Inc. [6], in which signal reflections occurred from strips printed on the surface of a piezoelectric material at different distances and hence different time separations are used for the encoding. SAW tag operates at 2.45 GHz and permits coding of 256 bits, which is comparable with the conventional RFID using an IC chip. This high coding capacity is possible because of the slow wave phenomenon in SAW. However, using conventional and low cost substrates producing a delay in the order of micro-seconds demands long transmission line. For 8 bit code, eight transmission line sections, each having a length of 180 mm, is used [7, 8].

Meandering can be conveniently used for reducing marge surface area [9–12]. However, in all cases, the coding capacity can be increased only by increasing the length of transmission line [13]. Moreover, fabrication of long delay lines within acceptable loss is a challenge. All the above techniques use only single frequency. The transmission lines used in these cases are not highly dispersive and hence the delay is independent of the frequency. Gupta et al. proved the use of C-sections in RFID applications [14].

In this paper we propose a chipless RFID using C-sections, which can operate in multi-frequency bands. The dispersive characteristics of C-sections are effectively exploited for this purpose. Highly dispersive transmission delay lines are used here so that signal at certain frequency can be delayed in a controlled manner which is independent from one frequency to another. A proof of concept for practical implementation of the tag is developed here. Each frequency band is directly related with the length of the C-sections. For the first time, the direct relation between the tag geometry and code is developed in a comprehensive way. If the ID is known, the tag geometry can be obtained directly from the tag ID and hence it is easy to implement. Contrary to [14], the structural and tag modes (back scattering response of C-sections which will be explained later) are used for the encoding.

Microstrip technology is used here, which enables direct printing of the structure. Moreover, narrow band multiple frequencies that

are compatible with ISM bands are employed. Additionally, the structure makes use of the coupling effect to increase the amount of delay, which miniaturizes the transmission line length in comparison to a linear or meandered transmission line. The authors already proved the concept of utilizing the group delay characteristics of microwave C-sections [15, 16]. However, this paper presents the experimental verification of the proposed tag mostly focused in a practical implementation point of view. For this, commercially available radar Novelda [17] is used. The results are compared with those obtained using Digital Oscilloscope and Vector Signal Generator, and a good agreement is obtained. One remarkable thing in this case is that a reference tag is not used and hence can avoid all the calibration techniques which make the whole system complex [1]. Moreover, the proposed tag can operate at N-frequencies (here $N = 2$) and explains a novel time-frequency encoding technique.

The paper is organized as follows. Section 2 depicts the operating principle. The design procedure of the proposed Chipless RFID system is explained in Section 3. Section 4 explains time domain measurement technique used without the need of a reference tag. The measurement results and simulation results are compared in Section 5 followed by conclusions.

2. OPERATING PRINCIPLE

The frequency dispersive property of transmission line can be utilized to rearrange different spectral components at different times. Frequency dispersion results from the propagation of different spectral components at different speeds. This characteristic is used for realizing chipless tags. Schiffman [18] made use of sections of the coupled transmission line (C-sections) to design broadband matched differential phase shifter in microwave region. Cristal [19] investigated the analytical properties of cascaded commensurate (equal length) transmission line C-sections and established a procedure for realizing the phase characteristics of these C-sections. Besides, Gupta et al. [20] presented a detailed study to find out the group delay characteristics of a cascaded non commensurate transmission line. A computer design approach had been used to obtain various group delay responses such as gaussian, linear and quadratic of the different C-section groups. However, here we simply seek to obtain peaks (preferably narrow) with significant group delay values. Commensurate C-sections are used with each group refers to a delay peak where the shape can be optimized by changing the number of C-sections or gap width.

Figure 1(a) depicts the operating principle of the proposed system

which comprises a chipless tag composed of two cross polarized broad band antennas and cascaded commensurate (equal length) C-section groups which forms the core of the system. The criteria for cascading the C-sections will be explained in the following section. The frequency dispersive characteristics of the microwave transmission line provides different spectral components rearranged in time and is utilized for encoding of chipless RFID tags. The group delay indicates time taken by a signal to propagate through a structure as a function of frequency.

For better understanding let us consider a system with N group of C-sections $C_1 \ldots C_i \ldots C_N$, where C_1 is the first group, C_i is an intermediate group and C_N is the last group. As shown in Figure 1(a), each group can have a finite number of lengths such as l_{11}, $l_{12 \ldots} l_{1n}$, where l_{1n} is the maximum length and l_{11} the minimum length of the C-sections for group C_1. The maximum length l_{1n} for a single C-section is directly linked to the fundamental frequency F_{C1} by the following relation:

$$F_{C1} = F(l_{1n}) \approx c/\left(4 * l_{1n}(\varepsilon_{eff})^{1/2}\right), \tag{1}$$

where ε_{eff} is the effective permittivity of the microstrip line and F_{C1} is the frequency at which the group delay is maximum, i.e., when the length of C-section is l_{1n}. As we will see in the following sections, for all other lengths, the group delay will be lower than this value. This relation is true in the case of a single C-section. When consecutive C-sections are cascaded, a negligible shift is observed in the frequency to the lower region because of the strong coupling between the C-sections, which increases the capacitive effect. This expression is used in the preliminary design. The lengths are further optimized by simulation. However, in order to allow the reader to have an idea of the system design, this expression is included here. In fact, the behavior here is similar to that of a microstrip coupler where the maximum coupling occurs under the same conditions.

Similarly for the group C_N, l_{Nn} is the maximum possible length of the C-sections among N different configurations at frequency F_{CN}. This allows a single tag to operate at multi-frequency. When this system is interrogated by a UWB compatible pulse, different commensurate group of C-sections modulate the interrogation signal in time and it backscatters the response which will be the sum of the response of each group of C-sections $C_1 \ldots C_i \ldots C_N$. Here, the backscattered signal which contains the ID of the tag will be the signal guided through the C-section and re-transmitted by the tag transmitting antenna.

The frequency F_{Cp}, where $p = 1 \ldots i \ldots N$, is geometrically related to the C-section as explained in Eq. (1). As already said, it is the

frequency at which the C-section with length l_{pn} produces a group delay peak and is assigned as the operating frequency for each group such as an ISM band. Later it will be shown that the group delay peaks for different C-section groups are independent of each other and can vary if and only if the length of the corresponding group is varied. This is the advantage of the C-section because of its dispersive property, which discriminates it from linear or meandered transmission line. In the case of linear or meandered line, any variation in length can cause a change in the total delay and will be independent of the frequency, which is the case for the entire existing time domain chipless RFID [7–13].

The filtered signal $S_{Cp}(t)$, the total signal reflected by the tag and arriving at the reader antenna, will consist of two components. The first component, the structural mode, is due to the reflection from the tag and is independent of the length of the C-sections. The second component, hereafter called as the tag mode, is a part of the signal guided through each group of C-sections and modulated in time at different frequencies and re-transmitted by the output antenna. This

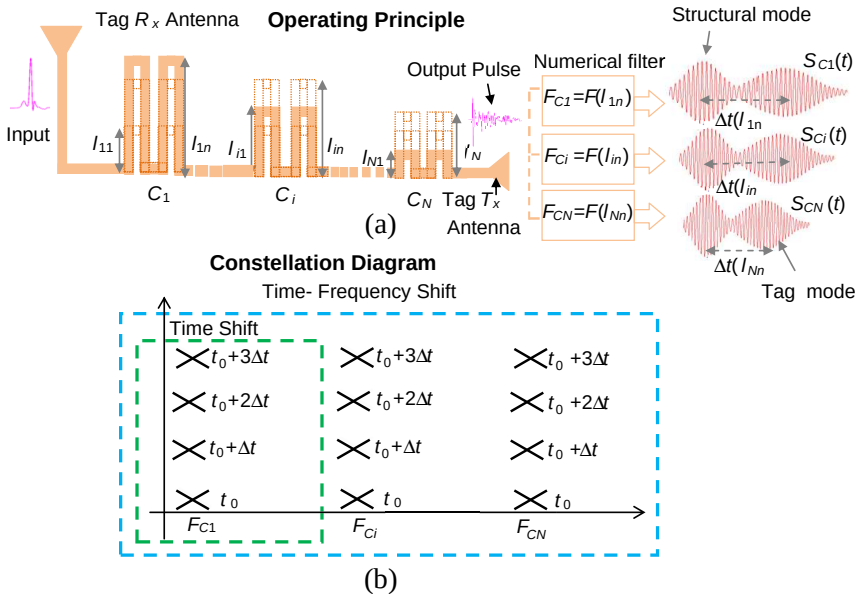

Figure 1. Proposed chipless RFID system along with the ID constellation diagram. (a) Operating principle. In the illustration each group consists of two C-sections. (b) Proposed time-frequency encoding principle.

will be explained in detail in the results and discussion sections. The time between structural mode and tag mode will be $\Delta t(l_{pn})$, which in turn corresponds to the group delay produced by the C-sections group with length l_{pn} and the delay produced by the two cross polarized antennas at the frequency F_{Cp} since the delay produced by other C-section groups at this frequency will be negligible. This re-transmitted signal will be sent back to the reader for decoding. The structural mode can be used as the reference and the time difference $\Delta t(l_{pn})$ between the structural mode and different tag modes can be used for generating different combinations of ID. Figure 1(b) shows the ID-constellation diagram corresponding to the new temporal multi frequency encoding technique. The following section explains the chipless RFID system design including the C-section design and UWB antenna design.

3. CHIPLESS RFID SYSTEM DESIGN

The tags were developed on Rogers R4003 ($\varepsilon_r = 3.55$, $\tan\delta = 0.0025$ and $h = 0.8\,\text{mm}$). Rogers were chosen instead of the low cost FR-4 substrate because of its low loss tangent which can enhance the back scattering characteristics of the tag. It was found in [15] that high loss tangent significantly reduces the amplitude of the tag modes. The chipless tag consists of two cross polarized UWB antennas, in between commensurate groups of C-sections are cascaded as shown in in Figure 2(b).

The tag antennas are cross polarized in order to reduce the interference between the interrogation signal and the backscattered signal which contains the tag information. Indeed, most of the objects

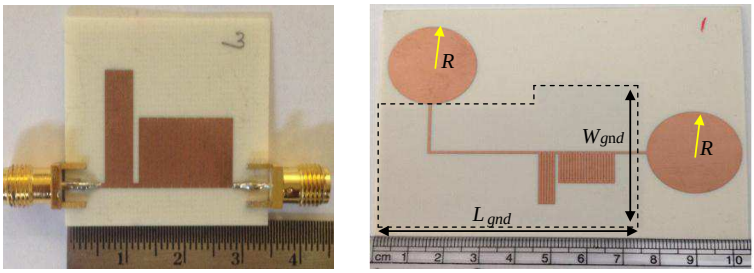

(a) (b)

Figure 2. Chipless tag comprises two groups of C-section; (a) prototype, (b) chipless tag; $g = 0.1\,\text{mm}$, $w' = w = 0.7\,\text{mm}$, $R = 13\,\text{mm}$, $L_{gnd} = 74.5\,\text{mm}$, $W_{gnd} = 47\,\text{mm}$; $\varepsilon_r = 3.55$, $\tan\delta = 0.0027$, $h = 0.8\,\text{mm}$. The lower ground plane is indicated by the dashed lines.

will reflect the signals with the same polarization and hence while labeling the tags, the reflections from any of the objects at a particular distance and a particular time may interfere with the tag information. A cross-polarization can avoid these problems. Indeed, a single antenna can also be envisaged instead of cross polarized antennas. A circularly polarized antenna with a matched load at the end of the C-section will cause the signal to travel through the C-section two times and leads to size reductions. Even though it improves the delay, the amplitude of the back scattered response of the C-section (tag mode) will be very low to detect. So two cross polarized antennas have been used to improve the system reliability. Further, unlike the chipless tags which do not have ground plane [1] and are very sensitive to surrounding objects, the proposed tag has ground plane which limits this problem. In the proposed case, it is mainly the adaptation level of tag antennas that may move, but their broadband characteristics make everything robust. Tests on plastic panels or glass were conclusive. CST Microwave Studio 2011 has been used as the simulation platform.

3.1. C-section Design

The C-section is the core of the proposed chipless tag, which is created by shorting the alternate ends of a coupled transmission line as shown in Figure 3(a) [16]. The group delay is the slope of the transmission phase response. It is obtained by taking the negative derivative of the phase with respect to the angular frequency. From the parametric

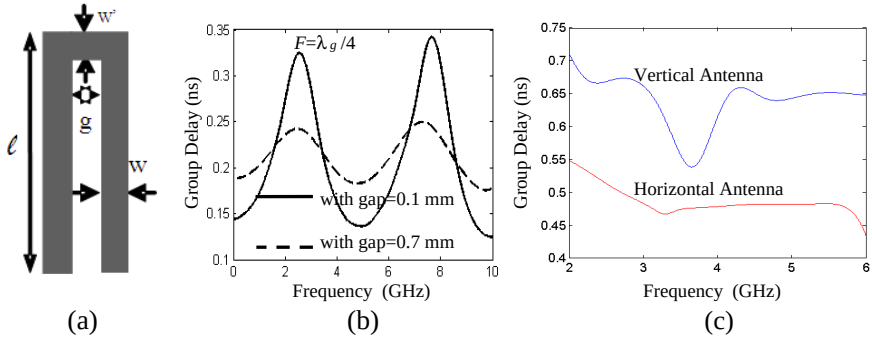

Figure 3. (a) Structure of the C-section with various parameters. (b) Periodic group delay curve for such a C-section with $l = 19.8\,\text{mm}$, which explains the effect of gap g and hence the coupling. (c) Simulated group delay curve for the vertical and horizontal antennas used (see Figure 2(b)); $w' = w = 0.7\,\text{mm}$; $\varepsilon_r = 3.55$, $\tan\delta = 0.0027$, $h = 0.8\,\text{mm}$.

study it has been found that the group delay increases with the decrease in the width and the gap of the lines in the C-sections. Decreasing the gap will also make the group delay curve narrower. It is evident from Figure 3(b) that the group delay is larger for smaller value of gap g since the coupling between each line increases with a decrease in the gap. As shown in the figure, group delay gives a maximum value for $l_{pn} = \lambda_g/4$, where λ_g is calculated using the effective permittivity ε_{reff} and defines the fundamental frequency as Eq. (1),

When several consecutive C-sections are cascaded together a small shift towards lower region is observed in the frequency, when the gap is very small. Due to the small gap coupling increases, the capacitive effect within the C-sections increases which in turn decreases the frequency. Also group delay increases with an increase in length and permittivity with a shift in frequency towards the lower region and will makes more frequency selective peaks.

Thus considering these aspects, the design parameters of the C-section have been determined and a prototype of the tag is designed as shown in Figure 2(a). Several C-sections with equal lengths have been added to increase the group delay. The width of the line is optimized as 0.7 mm which corresponds to the characteristic impedance of 82 Ω. Additionally, it is not necessary to design the width for 50 Ω; instead the width can be designed to match the input impedance of the antenna. The gap g has been assigned a value of 0.1 mm to provide tight coupling between the C-sections. As already explained decreasing the gap increases the group delay. However, due to fabrication limit the gap is limited to 0.1 mm and the number of C-sections was increased in order to have a significant delay. Also the gap's width w' is made equal to 0.7 mm to avoid any unwanted reflections due to impedance mismatch while integrating to the tag antennas. These design parameters are kept as constant and only the length of the C-sections has been changed for designing various tag configurations.

3.2. Criteria for Cascading the C-sections

As already mentioned, the group delay peaks are periodic and each peak can be varied by varying the length of the corresponding C-section as shown in Figure 4(a).

In order to increase the group delay, 3 C-sections are used here in a single group. As shown here, the group delay peaks are periodic and changing the length of the C-section will vary the group delay magnitude and frequency peak. However, for three groups of C-sections, there is a zone where the group delay variations are negligible even though the delay peaks are changing as marked in the figure. This zone, named as weak delay zone, has an importance while cascading

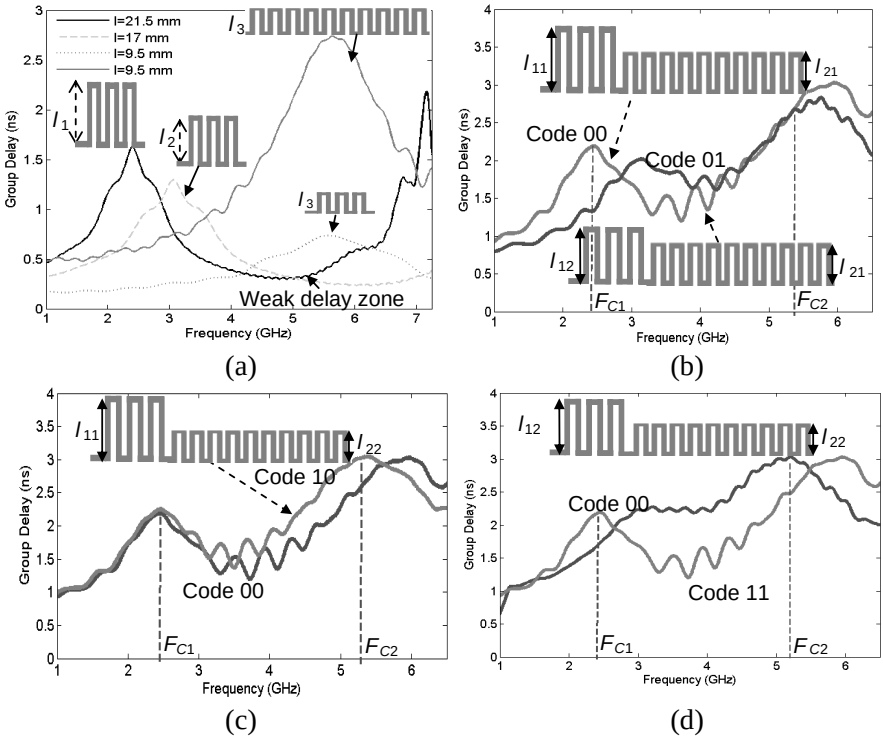

Figure 4. Principle of cascading C-sections. (a) Group delay peaks for different lengths of C-sections along with the cascading group delay curve produced by 10 C-sections. Group delay curve of cascaded C-sections corresponding to the code. (b) 00 & 01. (c) 00 & 10. (d) 00 & 11. Each time only the peaks corresponding to the change in length of C-section is varying making the other independent.

commensurate multi-group of C-sections. This zone permits the delay peaks for different lengths to be independent of each other. In this case, a second group can be added as shown in Figure 4(b). However, the most important feature of C-section which permits to cascade different groups and hence to produce different delay peaks is its dispersive nature. In the proposed tag, two groups of C-sections are used. Here in the second group, instead of three, ten C-sections are used because of two reasons (see Figure 4(b)). First, the value of delay will be less in high frequencies since the length of the C-section is small ($l_3 = 9.5\,\text{mm}$). Hence, while utilizing the same number of C-sections, the obtained delay will be very small to detect. Second, increasing the number of C-sections will increase the coupling between

C-sections and hence will make the group delay curve more selective in frequency as shown in Figure 4(a). However, more number of groups can be incorporated by increasing the coupling within each group so that the group delay peaks will be narrower resulting in a wide range of weak delay zone. This can be achieved by again increasing the number of C-sections in each group or by using multi-layer C-sections as explained in [21]. Thus, it permits the information encoding at several frequencies. Figures 4(b), (c) and (d) respectively represent the evolution of coding results from cascading two groups of C-sections.

3.3. UWB Antenna Design

The conventional disc monopole UWB antenna has been used as the tag antenna since it can operate in the desired frequencies [2]. Even though the operating frequencies of these tags are limited to one or more narrow bands, it was preferred to use broadband antenna in order to illustrate the frequency versatile characteristics of these tags. The antenna parameters are optimized to satisfy the operating frequencies of the tag and impedance matching with the tag. The width of the transmission line is kept as 0.7 mm to provide impedance matching to the C-section. The group delay of the vertically and horizontally polarized tag antennas has been simulated separately. The antennas were excited using waveguide port placed at the feed line, and 'far-field probes' (probes in CST which can be positioned outside the computation domain to record the electromagnetic far field) were placed at a distance, R [22]. Group delay of the transmission phase has been calculated by considering the phase of the reflected signal collected at the far-field probe. The corresponding group delay curves produced by the cross-polarized antennas are shown in Figure 3(c). The antennas produce a group delay. This was found not to be negligible (0.53 ns horizontally polarized antennas and 0.68 for vertically polarized antennas, thus 1.21 ns for the combination of the two antennas). Moreover, while integrating the antennas to the C-sections, it was found that the antennas modify the total group delay of the tag. In this context the authors were able to determine that the total group delay is the sum of group delays produced by the C-sections and the two tag antennas.

The following section of the article explains the time domain measurement techniques used. It explains the process utilized to separate the tag information.

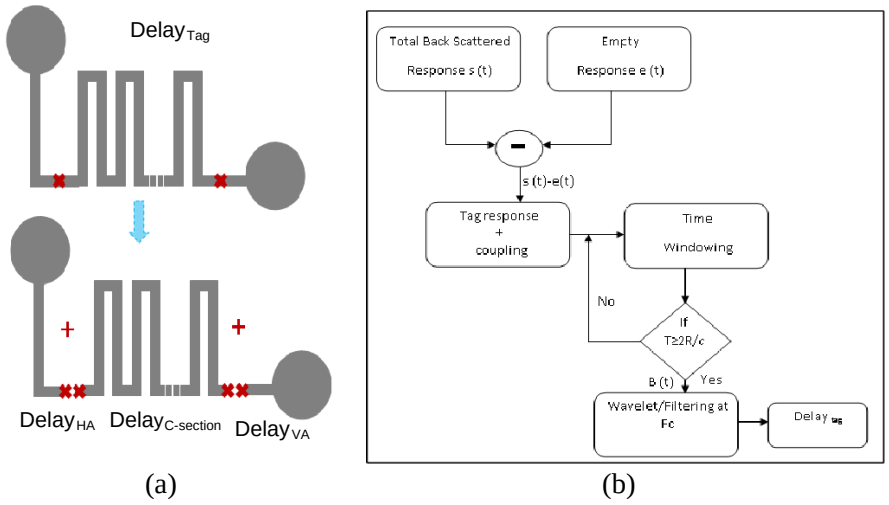

Figure 5. Principle used to extract the group delay and hence the tag information; (a) formulated conclusion, (b) process of information separation.

4. TIME DOMAIN MEASUREMENT TECHNIQUES

The most challenging part of the back scattering measurement is the information separation (delay produced by the tag), especially when the environmental delay has a predominant effect along with the delay produced by the tag.

Figure 5 explains the principle used to extract the group delay and hence the tag information. As we already explained, the back-scattered signal from the horizontally polarized tag antenna consists of structural mode and tag mode. The time Δt between these two modes is given by

$$\Delta t = \text{Delay}_{\text{tag}} = \text{Delay}_{\text{HA}} + \text{Delay}_{\text{C-section}} + \text{Delay}_{\text{VA}} + \text{Delay}_{\text{CA}}, \quad (2)$$

where Delay_{HA} is the delay produced by the horizontally polarized tag antenna and Delay_{VA} is that of the vertically polarized tag antenna. $\text{Delay}_{\text{C-section}}$ is the corresponding delay produced by the group of C-sections. Delay_{CA} is due to the coupling effect with the reader antenna, which is very weak (this feature will be shown in the following section) and hence one can consider the total delay as the sum of the first three parameters. It has been found that, the information separation can be done without the use of an additional reference tag. In all back scattering measurements, unwanted contributions can be found such

as reader antennas coupling and the contributions from RF cables, walls and other objects.

A background subtraction of the empty room response can eliminate all the unwanted contributions from the nearby objects, cables and antenna coupling, assuming that they are constant. Other parasitic effects can be eliminated by an efficient time windowing in the post signal treatment process [23]. Time windowing is interesting in practice since it can be used to extract the tag information directly without the use of a reference tag. Thus it reduces the need for reference tag measurement taking place with each tag combinations [1].

It has been found that when the distance between the tag and reader antenna increases, the time between the coupling signal to the reader antenna and the structural mode increases. It is in accordance with the equation $T = 2R/c$, where R is the distance and c is the speed of light in free space. The rising edge of the window can be determined from this equation while the falling edge can be determined by an optimization process, assuming that most of the decaying part of the signal is noise. Moreover, knowledge about the total tag response can also help to fix the falling edge. So in practice both edges were used in order to increase the robustness of the measurement. Figure 5(b) summarizes this process. The prototype and chipless RFID field trial results will be explained in the following section.

5. RESULTS AND DISCUSSION

5.1. Prototype Results

In order to prove the concept, 4 different variations have been considered. The lengths are optimized as 21.5 mm and 9.5 mm that correspond to ISM bands 2.45 GHz and 5.8 GHz respectively. The prototype with this configuration is chosen as the reference and the corresponding delay obtained has been assigned as the code '00'. The three other combinations were also designed by changing the length of the C-section. In the second combination, length l_{11} is changed to l_{12} by subtracting an amount of length Δl_1 and by keeping the length l_{21} as such. Similarly in the third combination, the length l_{21} is changed to l_{22} by adding an amount of length Δl_2 by keeping the length l_{11} as such. Finally both the lengths l_{11} and l_{21} have been changed to l_{12} and l_{22} and corresponding delay obtained has been assigned as the code 11.

Figures 6(c) and (d) show the simulated and measured group delay response of the cascaded commensurate multi group of C-section prototype as a two-port network. The two ports of the prototype have been connected to the Performance Network Analyzer (PNA N5222A). The delay produced by each prototype has been measured. As depicted

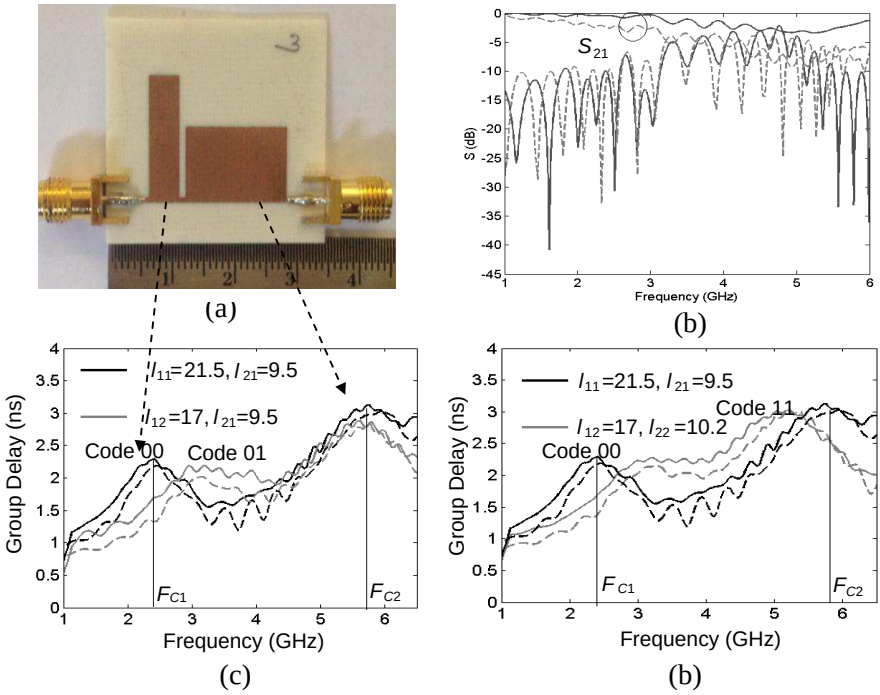

Figure 6. Results obtained along with the prototype. (a) Corresponding prototype. (b) Simulated (solid line) and measured (dashed line) S-parameter. Simulated (dashed line) and measured (solid line) group delay for two groups of C-section at two frequencies represent the evolution of different codes. (c) 00 & 01. (d) 00 & 11; $g = 0.1$, $w' = w = 0.7$; All the units are in mm. $\varepsilon_r = 3.55$, $\tan\delta = 0.0027$, $h = 0.8\,\text{mm}$.

in the figure, the two delay peaks are independent of each other and can be varied by changing the corresponding length of the C-section, which leads to different combination of tags. Thus in general the total number of peaks depends on the total number of C-section groups used.

Figure 6(b) shows the comparison between simulated and measured S-parameter curves. It is found that in measurement the amount of loss is higher than that of simulation. It may be due to the losses occurred while connecting a standard $50\,\Omega$ SMA connector to the designed $82\,\Omega$ feed line. However, the group delay is based on phase, which is independent of the magnitude variations; it doesn't reflect in the predicted group delay curves. This again proves the robustness of phase based encoding. As already stated, the group

delay peaks are periodic and each peak appears at odd multiple of frequency. This fact should be taken into account while designing tags for multiple frequencies. However, there is also the possibility of using the subsequent periodic harmonic while considering increasing the reliability of the reader. Thus the C-sections open a new path for temporal identification method for multi-frequency.

5.2. Chipless RFID System Field Trials

As shown in Figure 2(b), the prototype of the tag can be transformed into a chipless tag by adding a transmitting and receiving antenna at the two ends. The entire system was simulated and the backscattered signal from the receiving antenna was used for the encoding purpose. The simulated results and process of finding the time difference between structural and tag modes can be seen in [16]. For experimental validation, two horn antennas were used as the reader antennas, which are oriented in a cross-polarized form as shown in Figure 7(a). These horn antennas are separated by a distance of 10 cm and can operate within 700 MHz–18 GHz band with a gain of 12 dBi. The chipless tag and the reader antennas were placed at distance of 1.5 m. Both reader antennas and tags were mounted on plastic stands. A Gaussian signal with pulse width of 110 ps and maximum amplitude of 2 V generated by 'Picosecond 10060A' was used as the input for the system. The back scattered signal was measured using digital oscilloscope DSO91204A which is connected to the receiving horn antenna through an LNA (low noise amplifier). Contrary to [4], where LNA is not utilized in

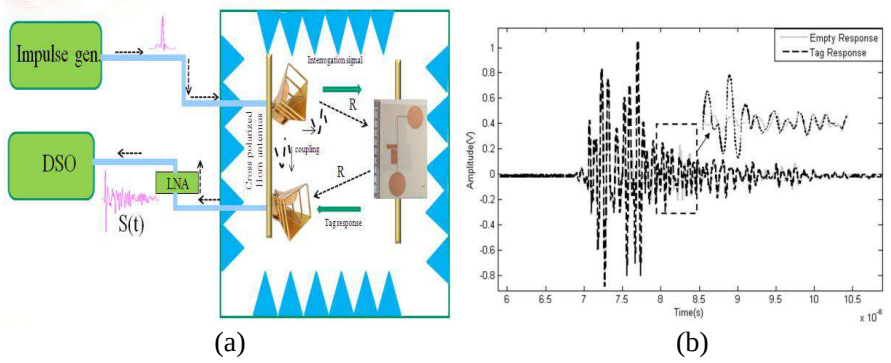

Figure 7. Experimental set up together with empty and tag responses. (a) Measurement set-up. (b) The measured empty response and tag response, insight view: zoomed version of the two responses.

the measurement and hence read range of 50 cm was obtained, in this measurement LNA has been used in the receiving end which enables read range of 1.5 m. The only measurement needed is the measurement for empty chamber and with tag, which is not difficult from a practical point of view. This is a prime advantage of the time domain and cannot be used in frequency domain where the amplitude of the signal (RCS) is used for the encoding. This again proves the robustness of temporal approach. Background subtraction has been done and a time windowing is applied as already explained. This background signal has a comparable magnitude with the scattering from the tag itself as shown in Figure 7(b). Thus an empty measurement (measurement without any tag) was done to perform the background subtraction. This time domain signal was subsequently subtracted from all other measurements for different chipless tags.

In order to separate the structural mode and different tag modes at the frequency of interest Continuous Wavelet Transform (CWT) is used [24]. The CWT performs a correlation analysis and as a consequence maximum output is expected when the input signal resembles the wavelet template. This input signal will be the time domain signature of the tag with amplitude in Volt. Consider the backscattered response of the tag after time windowing as $B(t)$ (see Figure 5(b)).

A Gaussian signal modulated at a carrier frequency of F_{C1} and F_{C2} is chosen as the known deterministic signal $p(t)$.

Thus,

$$P(t) = e^{-t^2/2t_v} \cos 2\pi F_{Ci} t,$$

where t_v is the time domain parameter which considers the bandwidth of the signal (BW = 0.1) and here $i = 1, 2$. Thus the wavelet template signal $p(t)$ is a signal which can be parameterized in frequency and bandwidth. A cross correlations of this signal with $B(t)$ has been done. Finally the maximum of this cross-correlation gives the unknown location parameter τ.

$$\tau = \max(B(t) * p(t)),$$

where $*$ represents the cross-correlation operation.

In our case, τ will be a combination of two peaks, the first peak represents the structural mode, and the second peak represents the tag mode. The difference between these two peaks gives the delay of the tag ($\text{Delay}_{\text{Tag}}$). This principle is the basis for a matched filter, which is the optimum detector of a deterministic signal in the presence of additive noise.

At each time, a Gaussian modulated signal at a carrier frequency of $F_{C1} = 2.45\,\text{GHz}$ and $F_{C2} = 5.8\,\text{GHz}$ respectively is used as the

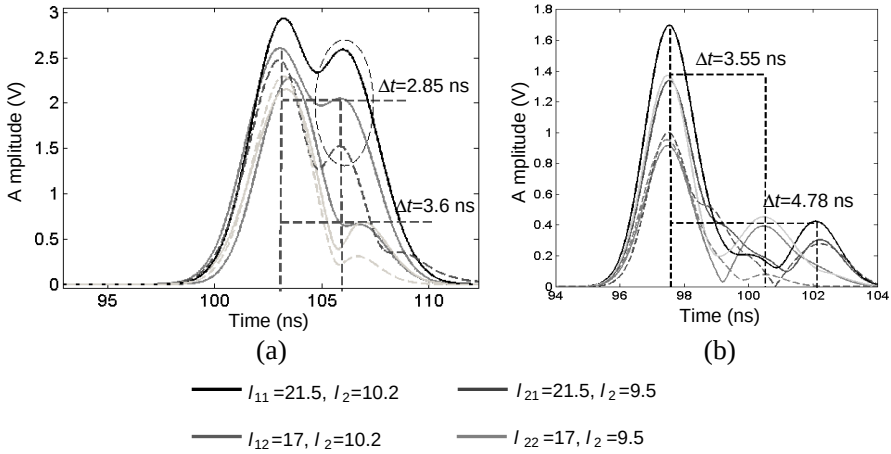

Figure 8. Measured delays for chipless tag with two groups of C-section; (a) at 2.45 GHz, (b) 5.8 GHz. Dashed line represents the response obtained from the commercial radar Novelda. Solid lines represent measurement using DSO and pulse generator. All units are in mm.

known deterministic signal. A cross correlation of the tag response with these modulated signals will result in two different peaks as shown in Figures 8(a) and (b). These measured delays at 2.45 GHz and 5.8 GHz respectively represent the corresponding binary code. First peak is the structural mode, which remains constant for all the tag combinations while the second component seems to be changing according to the length of the C-section. The delay between structural mode and tag mode will be the delay of the tag 'Delay$_{\text{tag}}$' and can be used for the encoding. It is clear from the figure that the delays are independent of each other and will change only with the length of the C-section. In all other cases it remains the same.

Table 1 gives the calculated, simulated, and measured delays obtained along with the delay produced by the UWB antennas at 2.45 GHz and 5.8 GHz. In this case the calculated delay is the sum of delay produced by cross-polarized antennas and C-sections at 2.45 GHz and 5.8 GHz respectively in simulation by using the Eq. (2).

Measurement was also done using commercially available UWB radar, Novelda (NVA6100) [17]. The radar is specified to be FCC compliant and to operate over a frequency range of 0.45 to 9.55 GHz with an averaging of 64 and a sampling rate greater than 30 Gs/s. To verify the characteristics of the radar, the emitted pulse has been measured and is able to detect tags up to 7 GHz.

Table 1. calculated, simulated and measured delays obtained.

$\text{Delay}_{\text{VA2.45 GHz}} + \text{Delay}_{\text{HA 2.45 GHz}} = 0.68\,\text{ns} + 0.53\,\text{ns} = 1.21\,\text{ns}$							
l_{11} (mm)	l_{21} (mm)	GD of C-section Sim. (ns)	Calc. Δt (ns) Simulation	Sim. Δt (ns)	Meas. Δt (ns) DSO	Meas. Δt (ns) Novelda radar	code
21.5	10.2	2.24	3.45	3.65	3.5	3.7	1
21.5	9.5	2.18	3.39	3.6	3.58	3.65	0
17	10.2	1.44	2.65	2.89	2.85	2.95	1
17	9.5	1.33	2.54	2.85	2.8	2.91	0
$\text{GD}_{\text{VA5.8 GHz}}+\text{GD}_{\text{HA5.8 GHz}} = 0.64\,\text{ns} + 0.47\,\text{ns} = 1.11\,\text{ns}$							
21.5	10.2	2.9	4.01	4.7	4.78	4.77	0
21.5	9.5	2.56	3.67	3.75	3.55	3.55	0
17	10.2	2.8	3.91	4.6	4.55	4.77	1
17	9.5	2.48	3.59	3.65	3.48	3.49	1

The dashed lines in Figure 8 represent the results obtained for each one of the combinations. As shown in figure, there is a good agreement with the results obtained using a Digital Oscilloscope and impulse generator. Table 1 shows a comparison of different delays obtained using Novelda and digital Oscilloscope. Contrary with the use of oscilloscope [4], it is essential to use a LNA with the radar Novelda to retrieve the ID of the tag correctly. This shows the limitations in terms of sensitivity of the radar. The maximum amplitude produced by Picosecond pulse generator is 2 V into a 50 Ω load giving a maximum instantaneous power of 19 dBm and that of Novelda is of the order of 200 mV.

The Federal Communications Commission (FCC) defines a power spectral density (PSD) of −41.3 dBm/MHz for the UWB band (3.1 GHz–10.6 GHz) [25]. If a CW signal is sent, it has to be very weak. But the possible way could be to develop an impulse radio based approach. In this case, a monocycle pulse of width lower than 100 ps is sent by the reader, but with a very low duty cycle. The minimum is 1 pulse/s (i.e., a duty cycle of 0.01%). European Telecommunication Standard Institute (ETSI) also allows the same PSD/MHz for the UWB band (3.1 GHz–4.8 GHz and 6 GHz–9 GHz). For ISM bands (2.4 GHz–2.4835 GHz), ETSI allows 10 mW (10 dBm) of e.i.r.p. (effective isotropic radiated power) for generic use. Thus, the allowed emission power is more in the case of ISM bands.

6. CONCLUSION & PERSPECTIVES

A novel encoding for chipless RFID based on temporal multi-frequency is proposed in this paper. The proposed tag can operate in ISM bands which permits the emission of more power making it suitable for applications where read-range is important. A good reading distance of 1.5 m is obtained with a UWB compatible pulse. The results in the real environment using commercial radar prove its importance in practical applications. This technique also proves the robustness of phase measurement and provides good results without a calibration tag. The robustness of the phase is the ability of phase to remain same in all environmental conditions. It has been proved experimentally in [2] that the phase information is more resilient to noise and can be read from a greater distance when compared to the amplitude information of the frequency signature. The multi frequency approach in time domain provides a new way of increasing coding capacity with a significant amount of delay. The size of the tag is more important now. This can be reduced by considering a more compact antenna, as the global size is due to the antenna sizes. Also techniques can be used to improve the amplitude of tag modes so that circularly polarized antennas can be used instead of the cross polarized one. Utilization of multi-layer design is also another solution. This will in turn increases the capacity of coding since more number of delay levels can be included instead of four as in the existing one. Because the delay peaks will be more selective in frequency for a multi-layer design. The number of C section groups can be increased to increase the capacity of coding. In this case, the structure should be more selective in frequency. As already explained multi-layer C-sections is a possible solution for this. The proposed paper thus proves the use of temporal multi frequency encoding in chipless RFID applications. Instead of two groups of C-section, cascading more number of groups of C-sections in a selective manner is also another way of increasing coding capacity. Another possibility is using the periodicity for coding the bits. For the moment the authors are mostly interested in the fundamental frequencies. These are the preliminary results obtained and the tag can be reproduced in a more efficient way. Also, methods are to be developed to bring the costs down for mass production, which may be possible by the use of flexible circuits like paper or PE which can reduce the cost of the tag significantly.

REFERENCES

1. Vena, A., E. Perret, and S. Tedjini, "Design of compact and auto compensated single layer chipless RFID tag," *IEEE Transactions on Microwave Theory and Techniques*, Vol. 60, No. 9, 2913–2924, 2012.
2. Preradovic, S., I. Balbin, N. C. Karmakar, and G. F. Swiegers, "Multi resonator based chipless RFID system for low cost item tracking," *IEEE Transactions on Microwave Theory and Techniques*, Vol. 57, No. 5, 1411–1419, May 2009.
3. Vena, A., E. Perret, and S. Tedjini, "Chipless RFID tag using hybrid coding technique," *IEEE Transactions on Microwave Theory and Techniques*, Vol. 59, No. 12, 3356–3364, 2011.
4. Vena, A., E. Perret, and S. Tedjini, "Novel compact RFID chipless tag," *PIERS Proceedings*, 1062–1066, Marrakesh, Morocco, March 20–23, 2011.
5. Vena, A., T. Singh, E. Perret, and S. Tedjini, "Metallic letter identification based on radar approach," *URSI GASS*, Istanbul, Turkey, August 13–20, 2011.
6. Hartmann, C. S., "A global SAW ID tag with large data capacity," *Proc. IEEE Ultrasonics Symp.*, 65–69, Munich, Germany, October 2002.
7. Zhang, L., S. Rodriguez, H. Tenhunen, and L. Zheng, "An innovative fully printable RFID technology based on high speed time-domain reflections," *Proc. of International Conference on High Density Microsystems Design and Packaging and Component Failure Analysis, HDP' 06*, Shanghai, China, June 27–30, 2006.
8. Zhang, L., S. Rodriguez, H. Tenhunen, and L. Zheng, "Design and implementation of a fully reconfigurable chipless RFID tag using Inkjet printing technology," *IEEE International Symposium on Circuits and Systems*, 1524–1527, May 2008.
9. Chamarti, A. and K. Varahramyan, "Transmission delay line based ID generation circuit for RFID applications," *IEEE Microwave and Wireless Components Letters*, Vol. 16, No. 11, 588–590, November 2006.
10. Shrestha, S., M. Balachandran, M. Agarwal, V. V. Phoha, and K. Varahramyan, "A chipless RFID sensor system for cyber centric monitoring applications," *IEEE Transactions on Microwave Theory and Techniques*, Vol. 57, No. 5, 1303–1309, May 2009.
11. Venmagiri, J., A. Chamarti, M. Agarwal, and K. Varahramyan, "Transmission line delay based radio frequency identification tag,"

Microwave and Optical Technology Letter, Vol. 49, No. 8, 1900–1904, August 2007.

12. Kalansuriya, P. and N. Karmakar, "Time domain analysis of a back scattering frequency signature based chipless RFID tag," *Proc. of Asia Pacific Microwave Conference (APMC)*, 183–186, Melbourne, Australia, December 2011.
13. Schubler, M., C. Mandel, M. Maasch, A. Giere, and R. Jakoby, "Phase modulation scheme for chipless RFID- and wireless sensor tags," *Proc. of APMC*, 229–232, 2009.
14. Gupta, S., B. Nikfal, and C. Caloz, "Chipless RFID system based on group delay engineered dispersive delay structures," *IEEE Antennas and Wireless Propagation Letters*, Vol. 10, 1366–1368, 2011.
15. Nair, R., E. Perret, and S. Tedjini, "Chipless RFID based on group delay encoding," *IEEE International Conference on RFID Technologies and Applications (RFID-TA)*, 214–218, Barcelona, Spain, September 2011.
16. Nair, R., E. Perret, and S. Tedjini, "Temporal multi-frequency encoding technique for chipless RFID applications," *IEEE MTT-S International Microwave Symposium IMS*, Montréal, Canada, June 17–22, 2012.
17. "Novelda nanoscale impulse radar," January 2013, Online Available: https://www.novelda.no/.
18. Schiffman, B. M., "A new class of broad-band microwave 90-degree phase shifters," *IRE Transactions of Microwave Theory and Techniques*, Vol. 6, No. 2, April 1958.
19. Cristal, E. G., "Analysis and exact synthesis of cascaded commensurate transmission-line C-section all-pass networks," *IEEE Transactions on Microwave Theory and Techniques*, Vol. 14, 285–291, June 1966.
20. Gupta, S., A. Parsa, E. Perret, R. V. Snyder, R. J. Wenzel, and C. Caloz, "Group delay engineered non-commensurate transmission line all-pass network for analog signal processing," *IEEE Transactions on Microwave Theory and Techniques*, Vol. 58, No. 9, 2392–2407, September 2010.
21. Settaluri, R. K., et al., "Design of compact multi-level folded line RF couplers," *IEEE Transactions on Microwave Theory and Techniques*, Vol. 47, No. 12, 2331–2339, December 1999.
22. Lam, H. J., Y. Lu, H. Du, P. M. Poman, and J. Bornemann, "Time-domain modeling of group-delay and amplitude characteristics in ultra wide band printed circuit antennas," *Springer Proc.*

in Physics, Vol. 121, 321–331, 2008.

23. Ramos, A., A. Lazaro, D. Girbau, and R. Villarino, "Time domain measurement of time-coded UWB chipless RFID tags," *Progress In Electromagnetic Research*, Vol. 116, 313–331, 2011.
24. Lazaro, A., A. Ramos, D. Girbau, and R. Villarino, "Chipless UWB RFID tag detection using continuous wavelet transform," *IEEE Antennas and Wireless Propagation Letter*, Vol. 10, 520–523, 2011.
25. Härmä, S., V. P. Plessky, X. Li, and P. Hartogh, "Feasibility of ultrawideband SAWRFID tags meeting FCC rules," *IEEE Trans. Ultrason., Ferroelect. Freq. Control*, Vol. 56, No. 4, April 2009.